

## On fluid modeling of Ion Temperature Gradient (ITG) driven modes

J. Zielinski<sup>1</sup>, A.I. Smolyakov<sup>1</sup>, P. Beyer<sup>2</sup>, M. Becoulet<sup>3</sup>,

G. Huijsmans<sup>4</sup>, X. Garbet<sup>3</sup>, S. Benkadda<sup>2</sup>

<sup>1</sup> University of Saskatchewan, Saskatoon, Canada

<sup>2</sup> Aix-Marseille Université, CNRS, PIIM UMR 7345, Marseille, France

<sup>3</sup> CEA/IRFM, Cadarache, France

<sup>4</sup> ITER Organization, Saint Paul Lez Durance, France

The Ion Temperature Gradient (ITG) mode plays a crucial role in the transport of ion energy in tokamaks. In addition, it is likely that ITG-driven turbulence is the main source for zonal flows and Geodesic Acoustic Mode (GAM) fluctuations, which are ubiquitous in tokamaks. A number of kinetic [1, 2] and fluid [3–5] models describing ITG modes have been studied in the literature. Many relevant simulations, using various numerical codes [6], have been targeted at such micro-turbulence studies, however these simulations are often performed in simplified geometry, or on restricted domains. Conversely, large-scale phenomena such as ELMs, low  $m$  magnetic perturbations, and shear flow structures are studied using different codes that take into account realistic plasma geometry, such as the divertor configuration, on a global domain. Nevertheless, there are explicit phenomena in each of these simulation regimes which are expected to be inherently coupled, eg. ITG turbulence driving large scale flows, low  $m$  magnetic islands affecting micro-stability via the modification of background profiles, etc. Therefore, it is important to describe these interacting phenomena using a single, coherent, framework.

JOREK [7], is a code which has been designed to study large-scale tokamak phenomena over a complete and realistic simulation domain. It solves a set of MHD-like equations in a finite-element framework, using third-order Bezier curves and implicit time stepping. These techniques are not restricted to the MHD equations, and thus other suitably formulated fluid models can be solved using JOREK’s framework.

The goals of the presented material are twofold. Primarily, we study JOREK’s capability for simulating ITG instabilities. To do this, we use a *base* two-fluid ITG model which is common in the literature [3–5]. We benchmark the resulting simulations against previous results attained within the linear regime [6]. Upcoming investigations on this front will proceed into the non-linear regime, then continue with the inclusion of more advanced profile and geometric effects. The eventual goal is to simulate zonal-flows and transport barrier formation, along with the subsequent L-H transition.

Concurrent to our simulation of the base model, we also develop an *advanced* ITG model,

which includes higher order terms, expected to produce results in closer agreement to kinetic theory. The base model accounts for the inertial/polarization terms in the ion density equation, and the divergence of the diamagnetic heat flux in the energy (balance) equation, however it neglects the polarization terms entirely in the energy equation. The advanced model incorporates the polarization terms into the energy equation at the same order as in the continuity equation, including inertial contributions to the heat flux. The higher order inertial velocity and heat flux terms are calculated by an asymptotic expansion in the low frequency approximation,  $\omega < \omega_{ce}$ . This procedure also involves the gyroviscous cancellation in both the energy and density equations, which allows the model to provide a consistent description of the ion Finite Larmor Radius (FLR) effects to a higher order than in the base model. These equations provide an asymptotically exact description of finite ion Larmor radius effects (FLR) in the limit of small  $k_\theta \rho_i$ . For large  $k_\theta \rho_i$ , this model reproduces the Pade-type approximants [8] to the Bessel function which are used in gyro-fluid models [9]. At the current time, this advanced model is only studied in the linear and local limit, however future studies will incorporate this model into JOREK as well, and study the difference in nonlinear ITG behavior.

To display the two sets of equations efficiently, we present the formulation of our adapted model, then identify the terms which are absent in the base model. We begin with the continuity equations for ions, under the condition of quasineutrality,

$$\frac{\partial n}{\partial t} + \nabla_\perp \cdot (n \mathbf{v}_\perp^{(0)}) + n_0 (\nabla_\perp \cdot \mathbf{v}_\perp^{(1)}) + \nabla_\parallel (n \mathbf{v}_\parallel) = 0, \quad (1) \quad \mathbf{v}_\perp^{(0)} = \frac{\hat{\mathbf{b}} \times \nabla \phi}{B} + \frac{\hat{\mathbf{b}} \times \nabla p_i}{enB}. \quad (2)$$

For the higher order terms, we use the gyroviscous cancellation [10] which results in:

$$\nabla \cdot \mathbf{v}_\perp^{(1)} = \nabla \cdot \left( \frac{\hat{\mathbf{b}}}{\omega_{ci}} \times \frac{d}{dt} \mathbf{v}_\perp^{(0)} + \frac{\hat{\mathbf{b}} \times \nabla \cdot \Pi_i}{enB} \right) \approx \nabla \cdot \frac{\hat{\mathbf{b}}}{\omega_{ci}} \times \frac{d_0}{dt} \mathbf{v}_\perp^{(0)} \approx -\rho_i^2 \nabla_\perp \cdot \frac{d_0}{dt} \nabla_\perp \left( \frac{e\phi}{T_{i0}} + \frac{p_i}{p_{i0}} \right), \quad (3)$$

where  $d/dt = \partial/\partial t + [(\mathbf{v}_E + \mathbf{v}_{pi} + \mathbf{v}_\parallel) \cdot \nabla]$ , and  $d_0/dt = \partial/\partial t + (\mathbf{v}_E \cdot \nabla)$ . After some algebra, we are left with the final form of our continuity equation,

$$\frac{\partial n_i}{\partial t} + \mathbf{v}_E \cdot \nabla n_i - 2n_i (\mathbf{v}_E + \mathbf{v}_{pi}) \cdot \nabla \ln B - n_0 \rho_i^2 \nabla_\perp \cdot \frac{d_0}{dt} \nabla_\perp \left( \frac{e\phi}{T_{i0}} + \frac{p_i}{p_{i0}} \right) + \nabla_\parallel (n_i \mathbf{v}_\parallel) = 0. \quad (4)$$

Parallel momentum balances are required, which are taken in the electrostatic limit as,

$$\frac{d_0 \mathbf{v}_\parallel}{dt} = -\frac{e}{m_i} \nabla_\parallel \phi - \frac{1}{nm_i} \nabla_\parallel p_i, \quad (5) \quad 0 = \nabla_\parallel \phi - \frac{T_e}{en} \nabla_\parallel n, \quad (6)$$

where we have ignored electron momentum and used  $\nabla_\parallel T_e = 0$ , since we are considering low frequency modes,  $\omega < v_{Te} k_\parallel$ , so the electron temperature is in equilibrium on flux surfaces.

The final governing equation is the ion energy balance,

$$\frac{3}{2} \frac{dp_i}{dt} + \frac{5}{2} p_i \nabla \cdot \mathbf{v}_i + \nabla \cdot \mathbf{q} + \Pi : \nabla \mathbf{v}_i = 0, \quad (7)$$

where  $\mathbf{v}_i = \mathbf{v}_{i\perp}^{(0)} + \mathbf{v}_{i\perp}^{(1)} + \mathbf{v}_{\parallel i}\hat{\mathbf{b}}$ , and we use the gyroviscous cancellation once more, leading to the same simplification as in (3), along with  $\nabla \cdot \mathbf{q} + \Pi : \nabla \mathbf{v}_i \rightarrow \nabla \cdot (\mathbf{q}^{(0)} + \mathbf{q}^{(1)})$  [10, 12]

$$\mathbf{q}^{(0)} = \frac{5}{2} \frac{cp_i}{eB_0} \hat{\mathbf{b}} \times \nabla T. \quad (8) \quad \mathbf{q}^{(1)} = \frac{1}{\omega_{ci}} \hat{\mathbf{b}} \times \frac{d_0}{dt} \mathbf{q}^{(0)} \approx -\rho_i^2 \nabla_{\perp} \cdot \frac{d_0}{dt} \nabla_{\perp} \left( \frac{T_i}{T_{i0}} \right). \quad (9)$$

Performing some algebra yields the final form of the ion energy equation,

$$\begin{aligned} \frac{\partial p_i}{\partial t} + \mathbf{v}_E \cdot \nabla p_i + \mathbf{v}_{\parallel i} \nabla_{\parallel} p_i - \frac{10}{3} p_i (\mathbf{v}_E + \mathbf{v}_{pi}) \cdot \nabla \ln B + \frac{5}{3} n_i \mathbf{v}_{Di} \cdot \nabla T_i + \frac{5}{3} p_i \nabla_{\parallel} \mathbf{v}_{\parallel i} \\ - \frac{5}{3} p_i \rho_i^2 \nabla_{\perp} \cdot \frac{d_0}{dt} \nabla_{\perp} \left( \frac{e\phi}{T_{i0}} + \frac{p_i}{p_{i0}} + \frac{T_i}{T_{i0}} \right) = 0. \end{aligned} \quad (10)$$

Thus, the *advanced* system consists of the four equations (4), (5), (6), and (10). The *base* system consists of the same equations, however ignores all Finite Larmor Radius (FLR) terms,  $\sim \rho_i^2$ , on the second line of the energy equation (10), and the pressure-dependent FLR term (containing  $p_i/p_{i0}$ ), in the continuity equation (4).

In order to simulate these equations in JOREK, we add artificial dissipation terms to equations (4), (5), and (10). The levels of dissipation are verified to cause no significant alteration of the mode frequencies in the region of interest,  $k_{\theta} \rho_i \lesssim 1$ . We use profiles suited to the standard *Cyclone* case [6], although the equilibrium Shafranov shift was artificially reduced to recreate an environment more similar to that of the flux-surface codes used in the comparison. Results from a particular ( $n = 30$ ) simulation are shown in figure 1. One can see that the poloidal location of the maximal mode envelope is rotated from the midplane by a ballooning angle,  $\theta_0 \sim 30^\circ$ . This rotation is found to decrease for smaller values of  $k_{\theta} \rho_i$ , at a constant  $\eta_i$ , and increase for a fixed  $k_{\theta} \rho_i$ , but decreased  $\eta_i$ . This is consistent with the behavior expected from studies of ballooning angle [11], and may result here due to the presence of equilibrium diamagnetic flows.

A series of simulations are performed using different toroidal harmonics,  $n$ , and perturbing the poloidal harmonic  $m = nq(r_m)$ , where  $q(r_m) \approx 1.45$  is measured at the location of maximum temperature gradient. This leads to growth rates and real frequencies plotted in figure 2, where we use  $k_{\theta} = m/r_m$ . Our results agree with those in [6] to within the deviations expected between flux-tube and global simulations. Specific differences originating from using the flux-tube equilibrium in [6] are discussed in [13]. Further skewing of the data can originate from the variation in the normalization values ( $\mathbf{v}_{Ti}$ ,  $L_n$ , and  $\rho_i$ ) over the global domain, and the use of  $k_{\theta} = m/r_m$ , when in reality a spectrum of  $m$  are excited.

Linear analysis of the base model, at the location of maximum temperature gradient, finds reasonably good agreement with the gyrokinetic results, as is also shown in figure 2. Inclusion of the higher order terms is found to make the mode unstable at significantly larger values of  $k_{\theta} \rho_i$ . This may be expected, since the model contains terms involved in both the toroidal ITG

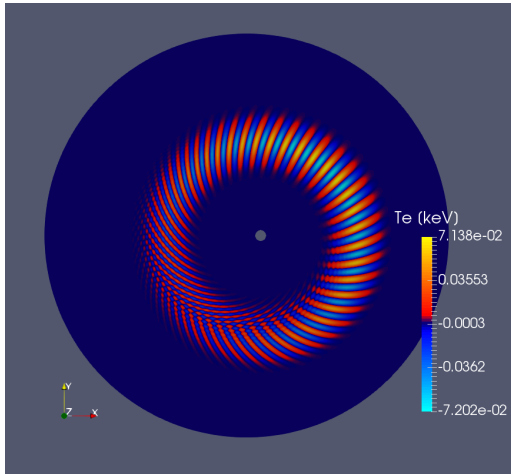


Figure 1: ITG mode in JOREK,  $n = 30 \rightarrow k_\theta \rho_i \approx 0.4$

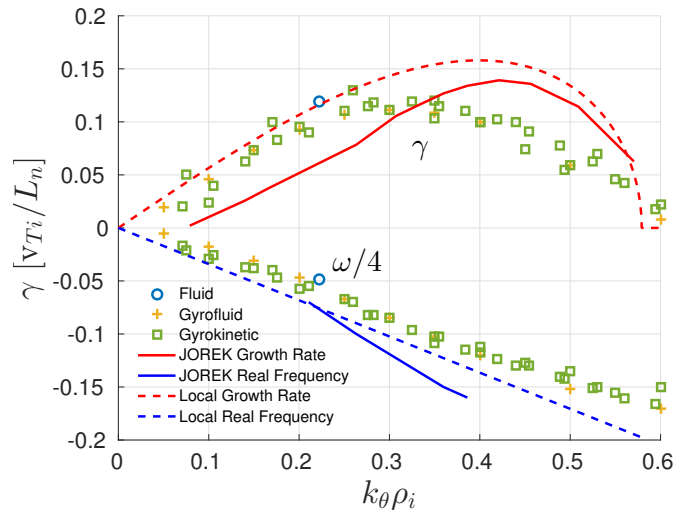


Figure 2: Growth rate and frequency of base model, compared to gyrokinetic results in [6]

(destabilization from magnetic curvature and gradients), and slab ITG (destabilization from finite parallel ion velocity). In linear analyses, the competition between these destabilization mechanisms may not be represented properly, and can lead to inaccurate results in wavelength regimes where there is competition between destabilization mechanisms, as is discussed for ballooning and interchange modes in [14]. This effect is expected to play a role here due to the competition of toroidal and slab ITG mechanisms for values of  $k_\theta \rho_i \sim 1$ . Further analysis of this behavior will be carried out using nonlinear simulations.

## References

- [1] B. Coppi, M. N. Rosenbluth, and R. Z. Sagdeev, *The Physics of Fluids* **10**, 3 (1967)
- [2] F. Romanelli and S. Briguglio, *Physics of Fluids B: Plasma Physics* **2**, 4 (1990)
- [3] Y. B. Kim, P. H. Diamond, H. Biglari, and J. D. Callen, *Physics of Fluids B: Plasma Physics* **3**, 2 (1991)
- [4] X. Garbet and R. E. Waltz, *Physics of Plasmas* **5**, 8 (1998)
- [5] S. Guo and J. Weiland, *Nuclear Fusion* **37**, 8 (1997)
- [6] A. M. Dimits, G. Bateman, M. A. Beer, B. I. Cohen, *et al*, *Physics of Plasmas* **7**, 3 (2000)
- [7] O. Czarny and G. Huysmans, *Journal of Computational Physics* **227**, 16 (2008)
- [8] B. N. Kuvshinov and A. B. Mikhailovskii, *Plasma Physics Reports* **22**, 6 (1996)
- [9] R. E. Waltz, R. R. Dominguez and G. W. Hammett, *Physics of Fluids B: Plasma Physics* **4**, 10 (1992)
- [10] A. I. Smolyakov, *Canadian Journal of Physics* **76**, 4 (1998)
- [11] R. Singh, S. Brunner, R. Ganesh, and F. Jenko, *Physics of Plasmas*, **21**, 3 (2014)
- [12] A. Brizard, *Physics of Fluids B: Plasma Physics* **4**, 5 (1992)
- [13] X. Lapillonne, S. Brunner, T. Dannert, S. Jolliet, *et al*, *Physics of Plasmas* **16**, 3 (2009)
- [14] B. D. Scott, *Physics of Plasmas* **12**, 6 (2005)